Journal of Statistical Physics manuscript No.
(will be inserted by the editor)

Renormalisation of 2D cellular automata with an absorbing state

Iain S. Weaver · Adam Prügel-Bennett

Received: date / Accepted: date

Abstract We describe a real-space renormalisation scheme for non-equilibrium probabilistic cellular automata (PCA) models, and apply it to a two-dimensional binary PCA. An exact renormalisation scheme is rare, and therefore we provide a method for computing the stationary probability distribution of states for such models with which to weight the renormalisation, effectively minimising the error in the scale transformation. While a mean-field approximation is trivial, we use the principle of maximum entropy to incorporate nearest-neighbour spin-correlations in the steady-state probability distribution. In doing so we find the fixed point of the renormalisation is modified by the steady-state approximation order.

Keywords renormalisation · cellular automata · statistical mechanics

PACS 05.10.Cc · 02.60.Cb · 05.70.Ln

1 Introduction

Cellular automata (CA) have become a staple component of many fields of computational research into spatially embedded interacting systems. Such systems consist of a coarse grid cells with both internal and local updating procedures. They have become a popular tool across a broad range of sciences and

This work was supported by an EPSRC Doctoral Training Centre grant (EP/G03690X/1).

Iain S. Weaver
School of Electronics and Computer Science, University of Southampton, University Road, Southampton, SO17 1BJ
E-mail: isw1g10@soton.ac.uk

Adam Prügel-Bennett
School of Electronics and Computer Science, University of Southampton, University Road, Southampton, SO17 1BJ

have found a plethora of applications from modelling free-way traffic flow to neuron activity (Nagel and Schreckenberg 1992; Ilachinski and Zane 2001).

While a wealth of research surrounds the study of equilibrium probabilistic cellular automata there is a relative paucity of work related to non-equilibrium CA in two-dimensions or more. Such models pervade almost all areas of science, from species distribution modelling to generating music (Balzter et al. 1998; Burraston and Edmonds 2005a,b). In this work we apply a real-space renormalisation to a binary two-dimensional PCA with an absorbing state, models which represent a $2+1$ dimensional directed percolation such as that shown in Fig. 1. This is a natural progression from the work of Edlund and Nilsson Jacobi (2010) who present a concise and systematic approach to renormalisation of such one-dimensional CA, which itself builds on previous work labelled as application of a dynamically driven renormalisation group (Toméand et al. 1997; De Oliveira and Satulovsky 1997). It is known that in applying some scale transformation to a CA, we do not guarantee the existence of an exact coarse grained dynamics, one which exactly incorporates all possible microscopic transitions. In such instances it is natural to choose the best fit by way of least-squares. The important contribution of Edlund and Nilsson Jacobi (2010) has been to show that what previously was referred to as the dynamically driven renormalisation group amounts to weighting this least-squares fit by the steady-state probability distribution such that error is concentrated on the transitions between relatively uncommon states.

We find a single fixed point in the renormalisation flow corresponding to the directed percolation universality class. As expected the fixed point of the renormalisation, the set of transition probabilities which are invariant with our scale transformation and therefore correspond to some scale-free critical dynamics, are adjusted by our estimate of the steady-state probability distribution of states used to weight the renormalisation. By applying the principle of maximum entropy we are able to surpass a mean-field steady-state to include nearest-neighbour spin-correlations. This method is in principle applicable to a wide range of CA of many states providing a well-defined transition matrix exists, although scaling ensures computational limitations will be reached quickly with increasingly complex CA.

We begin by briefly reintroducing the novel matrix representation of PCA transitions and states as used by Edlund and Nilsson Jacobi (2010) in Sec. 2. The corresponding real-space renormalisation algorithm is sufficiently general to treat PCA with any dimensionality and alphabet and is detailed in Sec. 3. As with previous work, coarse-grained degrees of freedom are insufficient to provide exact renormalisations, and therefore the best-fit renormalisation is found by the method of least-squares, which may be weighted by estimates of the stationary probability distribution of states whose computation is detailed in Sec. 4, along with an interpretation of the least squares fitting in terms of the dynamically driven renormalisation group (DDRG) in Sec. 5. The results of the renormalisation are given in Sec. 6 where we demonstrate the renormalisation flow in three dimensions along with the critical transition probabilities for

steady-state probability distribution estimates using mean-field and nearest-neighbour correlations.

2 Cellular Automata

We consider two-state PCA where lattice sites are denoted by either $\sigma \in \{\square, \blacksquare\}$. We denote the state of $n \times n$ blocks of lattice sites by the notation $\boldsymbol{\sigma}^n \in \{\square, \blacksquare\}^n$ whose probability distribution is held in the state vector $\boldsymbol{s}^n$ of length 2^{n^2}.

Transition probabilities of single site σ are goverened by the $k \times k$ block of sites in the previous interval and the transition matrix $\mathbf{P}$, which encompasses the microscopic dynamics of the PCA. $\mathbf{P}$ is a $2 \times 2^{k^2}$ transition matrix with elements $P(\sigma|\boldsymbol{\sigma}^k)$ giving the transition probability from a state $\boldsymbol{\sigma}^k \in \{\square, \blacksquare\}^k$ to the state $\sigma \in \{\square, \blacksquare\}$. In our notation so far, we can compute the single site probability distribution by applying the transition matrix

$$\boldsymbol{s}(t+1) = \mathbf{P}\boldsymbol{s}^k(t). \tag{1}$$

In order to update larger blocks of spins, we define a general transition probability matrix $\mathbf{P}^n$ which gives the probability vector $\boldsymbol{s}^n$ from its neighbourhood,

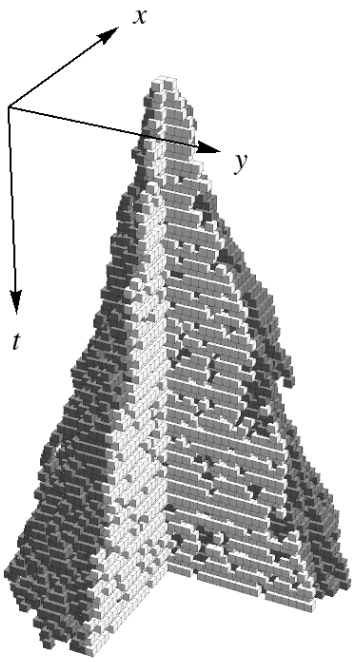

Fig. 1 A model of directed percolation initialised from a single seed in $2+1$ dimensions shown here above the critical point, where clusters grow and percolate through time. The lighter region shown a cross-section, indicating the cluster is not compact but contains holes, even in the case of the dense state being absorbing.

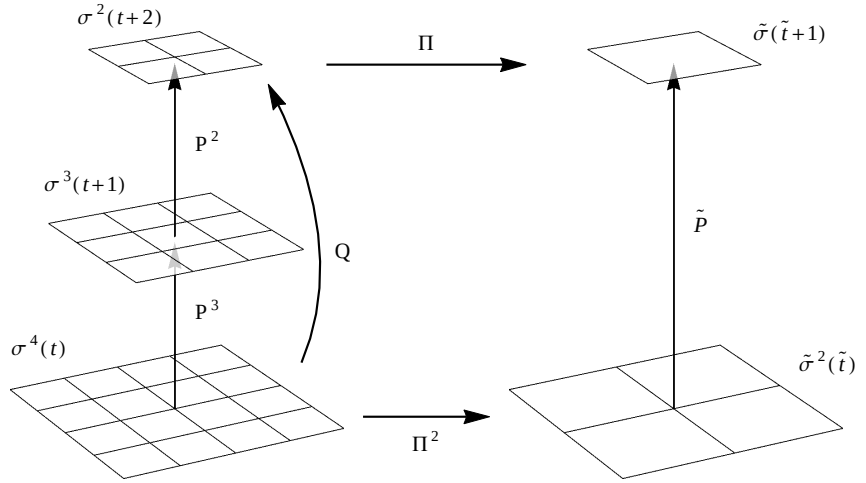

Fig. 2 The renormalisation algorithm for the $k = 2$ two-dimensional lattice. In the case of an exact renormalisation, the above matrices must commute; carrying out two timesteps through $\mathbf{Q} = \mathbf{P}^2\mathbf{P}^3$ followed by coarse graining by $\mathbf{\Pi}$ should be identical to beginning with the projection $\mathbf{\Pi}^2$, and applying the appropriate coarse-grained dynamics $\tilde{\mathbf{P}}$.

$\boldsymbol{s}^{k+n-1}$. For example, the transition matrix for a $k = 2$ PCA which maps blocks of spins of size $n + 1$ to n is

$$\boldsymbol{P}^n\left(\boldsymbol{\sigma}^n\middle|\,\boldsymbol{\sigma}^{n+1}\right) = \prod_{i,j=1}^{N} \boldsymbol{P}\left(\sigma^n_{i,j}\,\middle|\,\begin{matrix}\sigma^{n+1}_{i,j} & \sigma^{n+1}_{i+1,j}\\ \sigma^{n+1}_{i,j+1} & \sigma^{n+1}_{i+1,j+1}\end{matrix}\right). \tag{2}$$

In this work, we study PCA with an absorbing state, where the transitions from the vacuum state (all sites □) to any other state do not occur. In a binary PCA, such a model is expected to fall into the percolation universality class whose behaviour is illustrated by Fig. 1. As such, the large scale critical behaviour of these models is postulated to be universal, governed by a fixed point in the renormalisation flow which is attractive in the critical plane, precisely as illustrated for the case of one-dimensional PCA by Weaver and Prügel-Bennett (Weaver and Prügel-Bennett 2014).

3 Renormalisation Algorithm

The scale transformation begins with the coarse gaining projection $\mathbf{\Pi}$ which transforms the probability vector of blocks of N spins, $\boldsymbol{s}^N$, onto a single renormalised spin $\tilde{s}$

$$\tilde{s} = \mathbf{\Pi}\ \boldsymbol{s}^N \tag{3}$$

where $\mathbf{\Pi}$ is a $2 \times 2^{N^2}$ matrix with elements $\mathit{\Pi}(\tilde{\sigma}|\boldsymbol{\sigma}^N)$ giving the probability of projecting the state $\boldsymbol{\sigma}^N \in \{\square, \blacksquare\}^N$ onto $\tilde{\sigma} \in \{\square, \blacksquare\}$. In this work, we apply only the smallest trivial coarse graining $N = 2$. This spatial renormalisation

is accompanied by a stroboscopic renormalisation in time. Two updates can be carried out simply by taking the product of transition matrices

$$\mathbf{Q} = \mathbf{P}^2\mathbf{P}^{1+k}. \tag{4}$$

A coarse-grained dynamics $\tilde{\mathbf{P}}$ which, if it exists, satisfies the condition

$$\mathbf{\Pi}\ \mathbf{Q} = \tilde{\mathbf{P}}\ \mathbf{\Pi}^k. \tag{5}$$

where $\mathbf{\Pi}^k$ coarse grains $k \times k$ blocks of spins. Eq. (5) amounts to a statement that the coarse grained dynamics applied to the coarse grained projection of $\mathbf{s}^{2k}$ should be consistent with the microscopic dynamics, illustrated by Fig. 2.

4 Stationary Probability Distribution

When an exact solution to Eq. (5) does not exist, there is no macroscopic transition matrix which faithfully represents all allowed microscopic transition probabilities. In this instance we find the most representative renormalisation by way of a least-squares solution to Eq. (5). Previous work has shown the quality of the resulting renormalisation to be improved by incorporating the dynamics of the PCA, $\mathbf{P}$, referred to as the dynamically driven renormalisation group (Vespignani et al. 1996). In essence, the dynamics are utilised by taking a least-squares solution weighted by the stationary probability distribution of the $2k \times 2k$ spins at the microscopic level, shown in Fig. 2. The steady-state probability distribution satisfies the condition

$$\mathbf{P}^m \boldsymbol{s}_{\mathrm{st}}^{m+k-1} = \boldsymbol{s}_{\mathrm{st}}^m \tag{6}$$

where $\boldsymbol{s}_{\mathrm{st}}^m$ is the steady-state probability distribution of blocks of $m \times m$ lattice sites from which the larger distribution, $\boldsymbol{s}_{\mathrm{st}}^{m+k-1}$, must be *extrapolated* in a consistent way. For example, the first improvement which can be made over a mean field approximation considers only nearest-neighbour lattice correlations, illustrated in Fig. 3. Consistency with a $m = 2$ distribution $\boldsymbol{s}^2$ requires that the distribution $\boldsymbol{s}^3$ satisfies the constraint

$$\sum_{\sigma_1,\sigma_2,\sigma_3,\sigma_6,\sigma_9} s^3 \begin{pmatrix} \sigma_1 & \sigma_2 & \sigma_3 \\ \sigma_4 & \sigma_5 & \sigma_6 \\ \sigma_7 & \sigma_8 & \sigma_9 \end{pmatrix} = s^2 \begin{pmatrix} \sigma_4 & \sigma_5 \\ \sigma_7 & \sigma_8 \end{pmatrix} \tag{7}$$

for all configurations of $\boldsymbol{\sigma}^2$, a total of $2^4 = 16$ constraints of which 12 are unique (not related by lattice symmetry). These constraints may be written more conveniently as

$$\mathbf{C}\boldsymbol{s} = \boldsymbol{d} \tag{8}$$

where $\mathbf{C}$ is a sparse matrix with non-zero elements corresponding to the sum in the LHS of Eq. (7) and $\boldsymbol{d}$ is a vector with entries corresponding to the constraints in the RHS of Eq. (7). Extrapolation of one-dimensional probability distributions is trivial as there is only one extrapolated distribution consistent

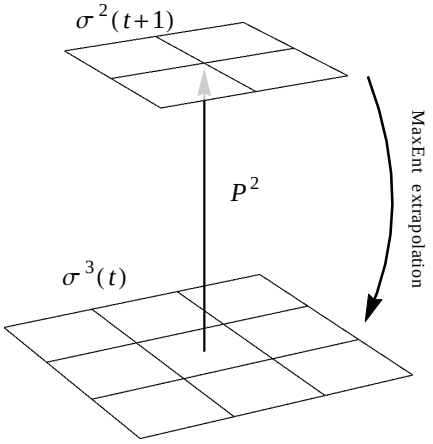

Fig. 3 A summary of the algorithm to compute the steady-state distribution $\sigma^2_{\rm st}$ which incorporates nearest-neighbour correlations. The solution in unchanged by an extrapolation $\text{ext}(\sigma^2_{\rm st} \to \sigma^3_{\rm st})$ followed by the transition matrix $\mathbf{P}^3$, the solution of Eq. (6).

with constraints which may be found by applying Bayes' theorem. However in two dimensions, there is no unique solution. We therefore search for the maximum entropy solution. Writing the Lagrangian

$$\begin{aligned}\mathcal{L}(\boldsymbol{\lambda}, \mu, s(\boldsymbol{\sigma})) = &- \sum_{\boldsymbol{\sigma}\in\boldsymbol{\sigma}'} D(\boldsymbol{\sigma}) s(\boldsymbol{\sigma}) \log(s(\boldsymbol{\sigma})) \\ &+ \sum_i \lambda_i \left(\sum_{\boldsymbol{\sigma}\in\boldsymbol{\sigma}'} s(\boldsymbol{\sigma}) C_i(\boldsymbol{\sigma}) - d_i \right) \\ &+ \mu \left(\sum_{\boldsymbol{\sigma}\in\boldsymbol{\sigma}'} D(\boldsymbol{\sigma}) s(\boldsymbol{\sigma}) - 1 \right) \end{aligned} \tag{9}$$

where $s(\boldsymbol{\sigma})$ and $D(\boldsymbol{\sigma})$ are the probability of configuration $\boldsymbol{\sigma}$ and its degeneracy (the number of equivalent constraints determined by the lattice symmetry) respectively, $\boldsymbol{C}(\boldsymbol{\sigma})$ and $\boldsymbol{d}$ contain the constraints and $\boldsymbol{\lambda}$ and μ are Lagrange multipliers, and sums are taken only over the unique configurations, $\boldsymbol{\sigma}'$, not related by lattice symmetry. Taking the derivative wrt. $s(\boldsymbol{\sigma})$

$$\frac{\mathrm{d}\mathcal{L}}{\mathrm{d}s(\boldsymbol{\sigma})} = -D(\boldsymbol{\sigma}) \log(s(\boldsymbol{\sigma})) - D(\boldsymbol{\sigma}) + \boldsymbol{C}(\boldsymbol{\sigma})\boldsymbol{\lambda} + \mu s(\boldsymbol{\sigma}) = 0 \tag{10}$$

Rearranging for $s(\boldsymbol{\sigma})$ gives the maximum entropy distribution as a function of the Lagrange multipliers and constraints

$$s(\boldsymbol{\sigma}) = \exp\left(\frac{\boldsymbol{C}(\boldsymbol{\sigma})\boldsymbol{\lambda}}{D(\boldsymbol{\sigma})} + \mu - 1 \right). \tag{11}$$

The normalisation parameter μ can be replaced simply by dividing through

by the partition function, $Z(\boldsymbol{\lambda})$

$$s(\boldsymbol{\sigma}) = \frac{1}{Z(\boldsymbol{\lambda})} \exp\left(\frac{\boldsymbol{C}(\boldsymbol{\sigma})\boldsymbol{\lambda}}{D(\boldsymbol{\sigma})}\right) \tag{12}$$

where

$$Z(\boldsymbol{\lambda}) = \sum_{\boldsymbol{\sigma}\in\boldsymbol{\sigma}'} D(\boldsymbol{\sigma}) \exp\left(\frac{\boldsymbol{C}(\boldsymbol{\sigma})\boldsymbol{\lambda}}{D(\boldsymbol{\sigma})}\right). \tag{13}$$

Substituting Eq. (12) into Eq. (9) gives the dual-objective

$$\begin{aligned}\mathcal{L}(\boldsymbol{\lambda}) =& -\sum_{\boldsymbol{\sigma}\in\boldsymbol{\sigma}'} D(\boldsymbol{\sigma}) s(\boldsymbol{\sigma}) \left(\frac{\boldsymbol{C}(\boldsymbol{\sigma})\boldsymbol{\lambda}}{D(\boldsymbol{\sigma})} - \log(Z(\boldsymbol{\lambda}))\right) \\ &+ \sum_{\boldsymbol{\sigma}\in\boldsymbol{\sigma}'} s(\boldsymbol{\sigma})\boldsymbol{C}(\boldsymbol{\sigma})\boldsymbol{\lambda} - \boldsymbol{d}\boldsymbol{\lambda} \\ =& \log\big(Z(\boldsymbol{\lambda})\big) - \boldsymbol{d}\boldsymbol{\lambda}\end{aligned} \tag{14}$$

whose minimum can be shown to satisfy the constraints

$$\begin{aligned}\frac{\mathrm{d}\mathcal{L}}{\mathrm{d}\lambda_i} &= \frac{1}{Z(\boldsymbol{\lambda})}\frac{\mathrm{d}Z}{\mathrm{d}\lambda_i} - d_i \\ &= \frac{1}{Z(\boldsymbol{\lambda})} \sum_{\boldsymbol{\sigma}\in\boldsymbol{\sigma}'} C_i(\boldsymbol{\sigma}) \exp\left(\frac{\boldsymbol{C}(\boldsymbol{\sigma})\boldsymbol{\lambda}}{D(\boldsymbol{\sigma})}\right) - d_i \\ &= \sum_{\boldsymbol{\sigma}\in\boldsymbol{\sigma}'} C_i(\boldsymbol{\sigma}) s(\boldsymbol{\sigma}) - d_i = 0.\end{aligned} \tag{15}$$

With the ability to extrapolate small blocks of spins to larger blocks we can solve Eq. (6) either through iteration or using normal root-finding methods. As with previous studies, we expect the accuracy of the renormalisation to improve with the quality of our estimate of the steady-state probability distribution $\boldsymbol{s}_{\mathrm{st}}$ which can be improved by accounting for longer range correlations in Eq. (6). Increasing the range, m, has been shown to give more representative weightings for the renormalisation and provides improvements in estimates of physical quantities such as the critical scaling exponent (Weaver and Prügel-Bennett 2014). As expected, increasing m in our two-dimensional implementation is very much limited by a computational ceiling, but also $m > 3$ results in Eq. (8) becoming rank-deficient and extrapolation cannot be performed in a consistent way as it can for $m \leq 3$. Additionally, the case of $m = 3$ poses other problems for certain coarse-graining projections as we will discuss shortly. For these reasons we limit the study to the cases of $m = 1$ *mean-field* and $m = 2$ *nearest-neighbour* correlations along with the unweighted $m = 0$ case.

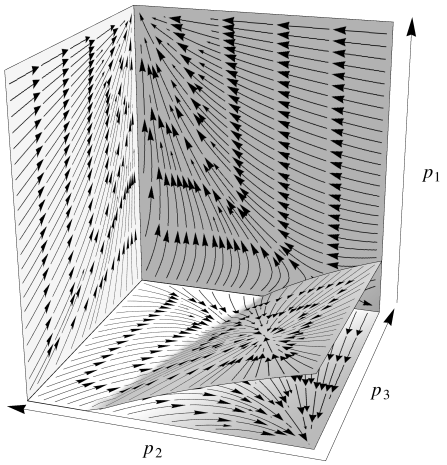

Fig. 4 The unweighted renormalisation flow of the across the surface of four intersecting planes with $p_2 = p_2'$ and $p_4 = 0.4502$. The curved plane is a projection of the critical plane and contains the critical point, illustrating that the point is attractive in this plane.

5 Least-squares

Having determined the stationary-distribution we seek a weighted least-squares solution to Eq. (5), achieved by defining the square error weighted by the probability vector $\boldsymbol{s}_{\rm st}^{2k}$

$$\mathcal{L}(\tilde{\mathbf{P}}) = \mathrm{Tr}\left(\boldsymbol{\Pi}\mathbf{Q} - \tilde{\mathbf{P}}\boldsymbol{\Pi}^k\right)\mathbf{D}\left(\boldsymbol{\Pi}\mathbf{Q} - \tilde{\mathbf{P}}\boldsymbol{\Pi}^k\right)^\top \tag{16}$$

where $\mathbf{D}$ is a diagonal matrix with the stationary probability distribution $\boldsymbol{s}_{\rm st}^{2k}$ along the diagonal. The solution is found where the derivative with respect to $\tilde{\mathbf{P}}$ to zero

$$\frac{\mathrm{d}\mathcal{L}}{\mathrm{d}\tilde{\mathbf{P}}} = 2\tilde{\mathbf{P}}\boldsymbol{\Pi}^k\mathbf{D}\boldsymbol{\Pi}^{k\top} - 2\boldsymbol{\Pi}\mathbf{Q}\mathbf{D}\boldsymbol{\Pi}^{k\top} = 0. \tag{17}$$

Solving for $\tilde{\mathbf{P}}$ we find

$$\begin{aligned}\tilde{\mathbf{P}} &= \boldsymbol{\Pi}\mathbf{Q}\mathbf{D}\boldsymbol{\Pi}^{k\top}\left(\boldsymbol{\Pi}^k\mathbf{D}\boldsymbol{\Pi}^{k\top}\right)^{-1} \\ &= \boldsymbol{\Pi}\mathbf{Q}\mathbf{D}^{\frac{1}{2}}\left(\boldsymbol{\Pi}^k\mathbf{D}^{\frac{1}{2}}\right)^\dagger\end{aligned} \tag{18}$$

where $\mathbf{A}^\dagger$ denotes the pseudo inverse $\mathbf{A}^\top(\mathbf{A}\mathbf{A}^\top)^{-1}$.

6 Renormalisation Flow

While the method we have presented is entirely general with respect to the size of the updating neighbourhood, k, both the computational and memory costs

Table 1 The critical transition probabilities estimated by our renormalisation group method where the renormalisation is unweighted, and weighted by approximations of the steady-state probability distribution considering only mean-field and nearest-neighbour spin-correlations.

Approximation	p_1	p_2	p_2'	p_3	p_4
Unweighted	0.1473	0.2664	0.2714	0.3677	0.4502
Mean-field	0.2703	0.4619	0.4667	0.6025	0.7031
Nearest-neighbour	0.2650	0.5150	0.4600	0.6888	0.8379

scale super-exponentially, and quickly become prohibitive. For this reason we limit ourselves to study symmetrical $k = 2$ transition matrices. This contains only five renormalisation parameters not related by lattice symmetry, which we label

$$\mathbf{P} = \begin{array}{c} \\ \square \\ \blacksquare \end{array} \begin{array}{c} \begin{array}{cccccc} \boxplus & \boxplus & \boxplus & \boxplus & \boxplus & \boxplus \end{array} \\ \begin{pmatrix} 1 & 1-p_1 & 1-p_2 & 1-p_2' & 1-p_3 & 1-p_4 \\ 0 & p_1 & p_2 & p_2' & p_3 & p_4 \end{pmatrix} \end{array}. \tag{19}$$

A coarse graining projection must be chosen which preserves the vacuum state in order that it be absorbing on all scales, that is to say it must never project a block of spins which contain a ■ onto a □. Therefore, the relevant projection is

$$\mathbf{\Pi} = \begin{array}{c} \\ \square \\ \blacksquare \end{array} \begin{array}{c} \begin{array}{cccccc} \boxplus & \boxplus & \boxplus & \boxplus & \boxplus & \boxplus \end{array} \\ \begin{pmatrix} 1 & 0 & 0 & 0 & 0 & 0 \\ 0 & 1 & 1 & 1 & 1 & 1 \end{pmatrix} \end{array}. \tag{20}$$

To visualise the flow of the five renormalisation parameters p_1, p_2, p_2', p_3 and p_4 we plot the hypersurface given by assuming a totalistic transition matrix $p_2 = p_2'$ with the transition probability p_4 taking its critical value in Fig. 4. The location of the critical point of the renormalisation group, the transition matrix which is invariant with our scale transformation, is shown for a range of steady-state approximations in Table 1. A comparison of these values to those produced from simulation of the PCA given by Eq. (20) may indicate the degree of improvement, if any, afforded by the range of approximation orders for the steady-state spin distribution. While properties such as the scaling exponent for clusters of spins have been found to a high degree of accuracy (Hinrichsen 2006), the location of the fixed point of the renormalisation is yet to be determined experimentally.

7 Conclusion

We have shown that the renormalisation algorithm used by Edlund and Nilsson Jacobi (2010) is sufficiently general to yield meaningful results when applied to two-dimensional PCA. To provide the dynamically driven component, an estimate of the stationary probability distribution of states, requires a unique *extrapolation* of a probability distribution over a small block of spins to a large one. In one-dimension, Bayes' theorem is sufficient though in two-dimensions

there is a hyper-surface of consistent extrapolated parameters and we employ the principle of maximum entropy to choose the configuration with the highest entropy, constrained by the requirement that our smaller probability distribution be recoverable. This has proven effective for $m = 2$ (to incorporate nearest-neighbour correlations into the steady-state distribution) though the method encounters unfortunate complications for the cases of $m = 3$ and $m \geq 4$. For $m = 3$, a steady-state including next-nearest-neighbour correlations, there is a transition to a vacuum steady-state whose volume is in disagreement with the dynamics of the renormalisation. A critical point could not be found when weighted with this approximation as it appears to lie within the range of renormalisation parameters in which the steady-state is expected to be a vacuum. On the other hand, in the case of $m \geq 4$ there is *no* consistent way to extrapolate the probability distribution consistently; the constraint matrix is rank deficient.

Unlike previous work relating to one-dimensional CA, an absorbing state is not necessary for the existence of large-scale structures. In one-dimension, if large structures are destroyed with a finite probability, there can be no structure on the very largest scales, and therefore only trivial fixed points in the corresponding renormalisation group. Two-dimensional systems do not have this quirk as the presence of a *hole* in a connected cluster does not destroy it, and indeed they may arise whether or not there exists an absorbing state. However, we find that applying a coarse graining projection where parity symmetry is preserved by probabilistic blocking, does not reveal any interesting fixed points in the renormalisation, rather there is a tendency towards unstructured apparently random behaviour on the large scale (ie: $p \to \frac{1}{2}$).

Previous work concentrated on determining the scaling behaviour at the critical point, estimated from the leading eigenvalues of the Jacobian at the critical point of the renormalisation (Weaver and Prügel-Bennett 2014). The quality of this approximation has been shown to be improved by increasing the range of interaction, the size of updating neighbourhood k, and by refining estimates of the steady-state distribution used to weight the renormalisation. For the one dimensional case, these refinements appear to yield significant improvement. In this case, we are severely limited by the computational complexity of the problem and are only able to produce very coarse estimates of the scaling exponent at the critical point (1.72,3.98,4.86 for our unweighted, mean-field and nearest-neighbour schemes respectively to be compared to the numerical estimate of 0.73 (Hinrichsen 2006)), and unable to comment on the improvement achieved by following the process through for larger updating neighbourhoods, or more accurate steady-state representations.

References

H. Balzter, P.W. Braun, W. Köhler, Cellular automata models for vegetation dynamics. Ecological Modelling **107**(2-3), 113–125 (1998). doi:10.1016/S0304-3800(97)00202-0. http://linkinghub.elsevier.com/retrieve/pii/S0304380097002020

D. Burraston, E. Edmonds, Cellular automata in generative electronic music and sonic art: a historical and technical review, in *Digital Creativity*, vol. 16, Citeseer, 2005a, pp. 165–185. Citeseer. doi:10.1080/14626260500370882. http://www.tandfonline.com/doi/abs/10.1080/14626260500370882

D. Burraston, E. Edmonds, Cellular automata in generative electronic music and sonic art: a historical and technical review. Digital Creativity **16**(3), 165–185 (2005b). doi:10.1080/14626260500370882. http://www.tandfonline.com/doi/abs/10.1080/14626260500370882

M.J. De Oliveira, J.E. Satulovsky, Renormalization group of probabilistic cellular automata with one absorbing state. Physical Review E **55**(6), 6377 (1997). doi:10.1103/PhysRevE.55.6377. http://link.aps.org/doi/10.1103/PhysRevE.55.6377

E. Edlund, M. Nilsson Jacobi, Renormalization of Cellular Automata and Self-Similarity. Journal of Statistical Physics **139**(6), 972–984 (2010). doi:10.1007/s10955-010-9974-z. http://link.springer.com/10.1007/s10955-010-9974-z

H. Hinrichsen, Non-equilibrium phase transitions. Physica A: Statistical Mechanics and its Applications **369**(1), 1–28 (2006). doi:10.1016/j.physa.2006.04.007. http://linkinghub.elsevier.com/retrieve/pii/S037843710600402X

A. Ilachinski, Zane, *Cellular Automata: A Discrete Universe* (World Scientific Publishing Co., Inc., River Edge, NJ, USA, 2001). ISBN 981238183X

K. Nagel, M. Schreckenberg, A cellular automaton model for freeway traffic. Journal de Physique I **2**(12), 2221–2229 (1992). doi:10.1051/jp1:1992277. http://www.edpsciences.org/10.1051/jp1:1992277

T. Toméand, M.J. de Oliveira, T. Tomé, Renormalization group of the Domany-Kinzel cellular automaton. Physical Review E **55**(4), 4000–4004 (1997). doi:10.1103/PhysRevE.55.4000. http://link.aps.org/doi/10.1103/PhysRevE.55.4000

A. Vespignani, S. Zapperi, V. Loreto, Renormalization of Nonequilibrium Systems with Critical Stationary States. Physical Review Letters **77**(22), 4560–4563 (1996). doi:10.1103/PhysRevLett.77.4560. http://link.aps.org/doi/10.1103/PhysRevLett.77.4560

I.S. Weaver, A. Prügel-Bennett, Renormalization group approach to 1D cellular automata with large updating neighborhoods. Complexity (2014). doi:10.1002/cplx.21557. http://dx.doi.org/10.1002/cplx.21557